Exchange effects and large angle proton scattering on light nuclei at intermediate energies: Formalism and application to $p + {}^4$He scattering

H. S. Sherif*
Nuclear Research Centre, University of Alberta, Edmonton, Alberta, Canada T6G 2N5
and Institute for Nuclear Theory, University of Washington, Seattle, Washington, 98195

M. S. Abdelmonem†
University of Petroleum and Minerals, Dhahran, Saudi Arabia
and Nuclear Research Centre, University of Alberta, Edmonton, Alberta, Canada T6G 2N5

R. S. Sloboda‡
Nuclear Research Centre, University of Alberta, Edmonton, Alberta, Canada T6G 2N5
(Received 29 November 1982)

The amplitude for elastic scattering of protons on a light nucleus is treated in a manner which takes into account the indistinguishability of the incident and target protons. We propose a simple model in which the direct and knockout amplitudes are represented by an optical potential amplitude. The rest of the exchange amplitude is cast in a form which represents the exchange of a heavy cluster between projectile and target; the heavy particle stripping amplitude. A modified distorted wave Born approximation appropriate for such elastic channel rearrangement is developed. This approximation simplifies the handling of finite range and recoil effects. The calculation of the heavy particle stripping amplitude requires knowledge of the proton-cluster overlap function of the target nucleus. The present model is applied to the scattering of protons on ^{4}He in the energy range 0.1–1.2 GeV. Several overlap functions derived from fits to the charge form factor of ^{4}He are used in the calculations. The general behavior of the large angle cross section is reproduced by our model. Of particular importance is the finding that the results are rather sensitive to the large momentum behavior of the overlap function. Moreover, functions that are derived from the charge form factor after correcting for meson exchange current effects appear to do better at higher energies than those with no correction. Good qualitative agreement with the 180° excitation function is obtained and the calculations predict a second shoulder near 1.1 GeV. We have also investigated the effect of the heavy particle stripping amplitude on the calculation of the large angle polarization.

[NUCLEAR REACTIONS Large angle $p + {}^4$He scattering ($T_p = 0.1$–1.2 GeV). Exchange effects, heavy particle stripping, modified DWBA. Calculated $\sigma(\theta), P(\theta)$. Compare different ^{4}He overlap wave functions.]

I. INTRODUCTION

One of the important contributions of the intermediate energy accelerators to nuclear studies has been the possibility of studying nuclear processes at high momentum transfer. This, of course, will have significant implications for our understanding of the nuclear wave functions. Among the processes studied are complex reactions such as pion production reactions and (p,d) type of pickup reactions, etc. The theoretical investigation of these reactions has already influenced in a serious fashion the way in which we handle the calculations of their amplitudes. In particular, it appears that relativistic effects play an important role in these reactions.[1,2] At the other end of the spectrum there have been several studies of seemingly rather simple processes such as proton elastic scattering on light nuclei. Some very interesting experimental measurements have been performed on the elastic scattering of intermediate energy protons on ^{3}He and ^{4}He nuclei, particularly at large scattering angles. An example of the wealth of physics contained in such data can be found in the intriguing structures observed in the 180° excitation functions.[3–5] Moreover, in some instances, such as in the case of $p + {}^4$He scattering, complete angular distributions for the cross section and analyzing power are available at several proton

energies.[6]

There has been a great deal of work on p-d scattering, both theoretical and experimental, at intermediate energies. However, this process is not covered by the present work; a discussion of recent developments in this subject has been given by Igo.[3] Our treatment here is more concerned with proton elastic scattering on light nuclei such as ^{3}He and ^{4}He. Several approaches have been developed in the recent past toward an understanding of the behavior of this process at large scattering angles. The majority of them are concerned with the particle exchange effects[7] resulting from the indistinguishability of the incident and target protons. Among these are calculations, based on the resonating group method, which have been successful in treating the scattering of protons on light systems in the energy range up to 150 MeV.[8] On the phenomenological level these exchange effects could be simulated through the addition of Majorana exchange terms to an optical potential.[9] Such an approach has met with some success in dealing with the behavior of the cross sections at large angles.[10–12]

In another approach the contribution of the triton exchange graph to backward $p + {}^4$He scattering was studied in the Born approximation and used to predict a strong dependence of the backward cross section on the incident energy.[13] Later Lésniak *et al.*[14] included absorption effects in this model, through the use of eikonal distorted waves, and found these to be important. The structure observed in the 180° excitation functions in both $p + {}^3$He and $p + {}^4$He scattering and particularly the change of slope observed in the former for proton energies in the range 400–600 MeV and 900–1300 MeV, and in the latter process in the energy range 200–400 MeV, has aroused interest in interpreting these as being due to the excitation of Δ resonances during the scattering process.[4]

In this paper we give the details of a model which was outlined earlier in Ref. 15. This model, similar to the work of Refs. 13 and 14, is based on particle exchange effects as the major contributor to backward scattering. The present approach differs from earlier works in the following main respects.

(i) The contribution of the direct part of the scattering matrix is included in the calculations.

(ii) We introduce a modified distorted-wave Born approximation (DWBA) for treating the rearrangement amplitude.

(iii) Optical model distorted waves are used in the calculations with full account for spin-orbit distortions.

(iv) We discuss in more detail the role of the target wave function in the calculations and show how the behavior of the cross section at large angles is sensitive to the large momentum behavior of the overlap wave function.

This model is applied here to $p + {}^4$He scattering in the energy range 0.1–1.2 GeV. A reasonable account for the observed large angle cross section is obtained. We find that at higher energies overlap functions that are derived from the charge form factor, after taking into account the meson exchange current effects, generally lead to better agreement with the large angle data than those that neglect these effects. We show that this is intimately related to large differences among these functions at high momenta. Reasonable agreement with the 180° excitation function is obtained and a second shoulder is predicted near 1.1 GeV. The inclusion of the HPS mechanism is found to improve the large angle polarization at 147 MeV. At higher energies, however, one is not yet able to get a good agreement with the measured polarizations at large angles. In a subsequent paper the model will be applied to the $p + {}^3$He process.

In Sec. II we give the basic ingredients of the model and carry out some details of the calculations as they apply to the $p + {}^4$He case. In Sec. III we present the comparison of our results with experiments and discuss in some detail the role of the target wave function as it is derived from the charge form factor and the effect of allowing for meson exchange currents. A conclusion is given in Sec. IV.

II. FORMALISM

Consider the elastic scattering of a proton on a light target nucleus which has n_p protons. When exchange effects between the target and projectile protons are taken into account, the elastic scattering t matrix can be written as[16]

$$T = T_{\mathrm{D}} - n_p T_{\mathrm{EX}} \tag{1}$$

where T_{D} and T_{EX} are the direct and exchange matrix elements, respectively. The latter, of course, refers to the situation where the outgoing proton is one of the target nucleons. There are two mechanisms through which this can be accomplished, namely, the knockout (KO) and the heavy particle stripping (HPS) mechanisms.[17] These are illustrated by the diagrams in Fig. 1. Equation (1) can thus be rewritten

$$T = T_{\mathrm{D}} - n_p T_{\mathrm{KO}} - n_p T_{\mathrm{HPS}} \, . \tag{2}$$

Because it is likely that the KO term will generally, like the direct one, be forward peaked we combine these together in one term. The first ingredient of our present model is to represent this term by an optical potential t matrix. The justification for this is in the fact that the emphasis of the present study is

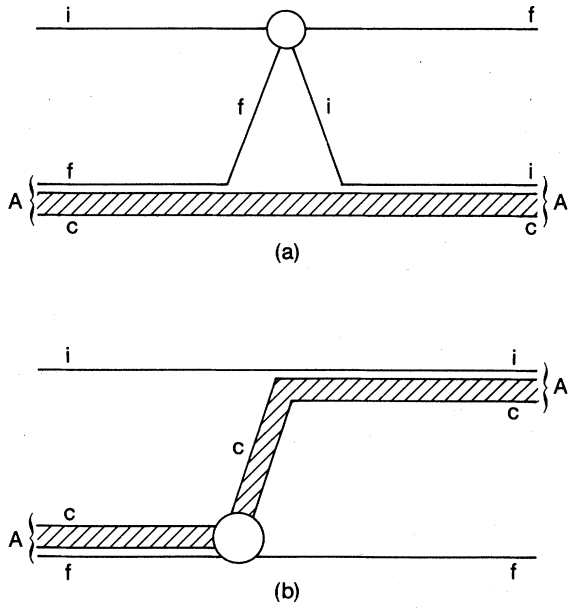

FIG. 1. Schematic diagrams of rearrangement scattering. (a) The knockout mechanism. (b) The HPS mechanism. The blob denotes the interaction responsible for the particular rearrangement.

on investigating the role of the heavy particle stripping term and, hence, we wish to have as simple a description as possible of the other two matrix elements. The optical potential provides us with this as well as with a reasonably good account of the forward angle data. We, therefore, rewrite Eq. (2) as

$$T \simeq T_{\mathrm{OPT}} - n_p T_{\mathrm{HPS}} \ . \tag{3}$$

T_{OPT} is calculated in the usual manner from an optical model (OM) potential. In the following we give details of our calculations of T_{HPS}.

If the target nucleus is regarded as being made up of a core cluster c plus a proton f and if i denotes the incident proton, then the exact expression for the HPS t matrix is

$$T_{\mathrm{HPS}} = \langle e^{i\vec{k}_f\cdot\vec{r}_f}\Phi(i,c) \mid V_{fc} \mid \Psi^{(+)}(i,f,c)\rangle \ . \tag{4}$$

$\Phi(i,c)$ is the target wave function in the final state, made up of proton i and cluster c, V_{fc} is the interaction potential of proton f with cluster c, and the wave function $\Psi^{(+)}(i,f,c,)$ is the total wave function of the system with appropriate boundary conditions. For the moment, spin indices are suppressed for simplicity. We approximate $\Psi^{(+)}$ in the usual way by the product of the target wave function $\Phi(f,c)$ and an optical potential distorted wave $\chi^{(+)}(\vec{k}_i,\vec{r}_i)$ describing the motion of proton i relative to the center of mass of the target.

Our expression for T_{HPS} then becomes

$$T_{\mathrm{HPS}} = \langle e^{i\vec{k}_f\cdot\vec{r}_f}\Phi(i,c) \mid V_{fc} \mid \Phi(f,c)\chi^{(+)}(\vec{k}_i,\vec{r}_i)\rangle \ . \tag{5}$$

The distorted wave $\chi^{(+)}$ is generated using the same optical potential used to calculate T_{OPT}.

The above expression is our distorted-wave Born approximation for T_{HPS}. It is different from the usual DWBA expression in that the outgoing channel is represented by a plane wave. The origin of this difference is due to the fact that we are dealing with a rearrangement leading to the elastic channel and, hence, the usual practice[18] of adding and subtracting an exit channel optical potential (from which the outgoing distorted wave is generated) is not applicable. One must also add that the presence of a plane wave in the exit channel does indeed make it easier to handle both finite range and recoil effects.

A. The $p + {}^4\mathrm{He}$ case

We now consider the calculation of the HPS amplitude for the specific case of proton scattering on ^{4}He. The target is considered to be made up of a triton cluster t and proton f. The spin structure in this case is simple and the internal space wave function is an s state. Likewise, in the final state, the ^{4}He nucleus contains proton i and triton t. Assuming the interaction V_{ft} to be free of any explicit spin dependence, after some simple spin algebra is carried out one gets

$$T_{\mathrm{HPS}} = \tfrac{1}{2}\langle e^{i\vec{k}_f\cdot\vec{r}_f}\psi(r_{it}) \mid V(r_{ft}) \mid \psi(r_{ft})\chi^{(+)}_{\mu_i\mu_f}(\vec{k}_i,\vec{r}_i)\rangle \ , \tag{6}$$

where the subscripts μ_i and μ_f refer to the initial and final proton spin projections, respectively, and $\psi(r)$ is the radial overlap function.

In an earlier short account of this work,[15] we showed how the use of the spherical δ-shell approximation[19] can simplify the six-dimensional integrals on the right-hand side (RHS) of Eq. (6). This approximation works well up to proton energies near 200 MeV. We shall not use it in the present treatment, but rather will carry out full finite range calculations since we wish to apply the model at higher proton energies. We choose as integration variables the coordinates $\vec{r}_i$ and $\vec{r}\equiv\vec{r}_{ft}$ and express the other coordinates appearing in Eq. (6) in terms of these (see Fig. 2):

$$\vec{r}_{it}=\vec{r}_i+\frac{m_p}{M_H}\vec{r}\simeq\vec{r}_i+\tfrac{1}{4}\vec{r}$$

and (7)

$$\vec{r}_f=\vec{r}-\frac{m_p}{M_H}\vec{r}_{it}\simeq\tfrac{15}{16}\vec{r}-\tfrac{1}{4}\vec{r}_i\ ,$$

$$T_{\rm HPS}=\tfrac{1}{2}\int d\vec{r}_i e^{i(1/4)\vec{k}_f\cdot\vec{r}_i}\left[\int d\vec{r}e^{-i(15/16)\vec{k}_f\cdot\vec{r}}\psi(|\vec{r}_i+\tfrac{1}{4}\vec{r}|)\left[\frac{\hbar^2}{2m}\nabla^2-\epsilon_b\right]\psi(r)\right]\chi^{(+)}_{\mu_i\mu_f}(\vec{k}_i,\vec{r}_i)\ , \quad (8)$$

where m is the proton-triton reduced mass and ϵ_b is the proton-triton relative binding energy in the ^{4}He. The specific choice of the wave function ψ will be based on consideration of the ^{4}He charge form factor as determined from electron elastic scattering. This is discussed in Sec. II A 1. For now we need only to state that the function ψ is written as a sum of exponentials:

$$\psi(r)=\frac{e^{-\alpha r}}{r}\sum_{j=1}a_j e^{-\beta_j r} \quad (9)$$

which reduces asymptotically to $\sim e^{-\alpha r}/r$ (where $\alpha^2=2m\epsilon_b$). This particular choice of the wave function simplifies somewhat the evaluation of the integrals in Eq. (8). These are now carried out by expanding the plane waves and the distorted wave into sums of partial waves. The only remaining difficulty lies in the wave function $\psi(|\vec{r}_i+\frac{1}{4}\vec{r}|)$ which is made up, according to Eq. (9), of sums of exponentials. Each exponential term is expanded in terms of appropriate spherical harmonics and modified Bessel functions. The integrations are then evaluated numerically.

1. The ^{4}He wave function and meson exchange current effects

The wave function ψ describing the p-t relative motion in ^{4}He is determined from considerations of the ^{4}He charge form factor.[20,21] Some authors[14,22] have successfully found simple wave functions that fit the measured form factor $F_c(q)$. In recent years, it has become evident that one must make allowances for meson exchange current contributions to $F_c(q)$, before determining ψ. This is particularly relevant in the domain of intermediate energy nuclear reactions where one generally probes the high momentum components of the wave function. An example of this can be found in the work of Shepard *et al.*[23] on (p,d) reactions on ^{4}He. A similar investigation has been carried out for the ^{4}He$(p,2p)^3$H reaction by van Oers *et al.*[24] We shall investigate here the impact of using two kinds of wave functions: those which do not take into account the meson exchange current effects on the charge form factor (NOMEC) and those that do (MEC). We shall see that the results obtained with the latter are superior particularly at higher energies.

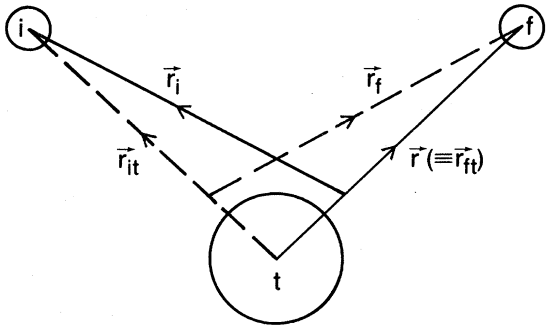

FIG. 2. Relative coordinates.

Lim[22] has suggested the use of an Eckart type of wave function for $\psi(r)$ and obtained a generally good fit to the observed ^{4}He charge form factor. Later, Lésniak *et al.*[14] managed to improve the fit by selecting slightly different parameters. We adopt their wave function to represent the class of function based on the form factor with NOMEC. We shall refer to this function as ECKART4. It is given by

$$\psi_{\rm ECKART4}(r)=\frac{N}{r}e^{-\alpha r}\left[1-e^{-\beta r}\right]^n \quad (10)$$

with $\beta=1.42$ fm^{-1} and $n=4$.

The MEC contributions to $F_c(q)$ for several nuclei have been calculated by Gari *et al.*[25] These authors point out that their calculations for ^{4}He are reliable up to $q=4$ fm^{-1}. Shepard *et al.*[23] have used the calculated meson exchange corrected form factor to determine a relative motion wave function where the internal part is based on a $(1s)^4$ configuration for ^{4}He. Their wave function is finite at the origin; its behavior at short distance is more or less Gaussian. On the other hand van Oers *et al.*[24] and later Greben[26] followed a somewhat different procedure in which the MEC corrected form factor is obtained by subtracting the theoretical meson exchange contribution[25] from the experimental charge form factor.[20,21] These authors then used this to determine the

parameters a_j and β_j of a relative wave function of the type given by Eq. (9). In this work we use the wave function given by van Oers *et al.*[24] in some of the comparisons given in the next section. We refer to this function as EXP2. Its parameters are given in Table I. The wave function given by Greben[26] turned out to yield results that differ only slightly from those obtained using the EXP2 overlap function.

We have also investigated two other functions that are based on MEC. One of these is of the Eckart type with $n=3$ (referred to here as ECKART3). This function provides a reasonably good fit to the corrected form factor up to $q=4$ fm^{-1}. It is used here as part of the illustration of the impact of the high momentum behavior of the wave function on our calculations.

As mentioned above, Shepard *et al.*[23] used a wave function which is finite at the origin, whereas all the above-mentioned wave functions vanish at the origin. We have derived a wave function EXP1 of the form used in Eq. (9) which is constrained to be finite at the origin and to fit the corrected form factor due to Greben[26] up to q slightly above 4 fm^{-1}. The parameters of the function were first started by fitting the radial wave function provided by Shepard *et al.*[23] and then were further refined to fit the form factor.

In Table I we give the parameters of the above wave functions. The Eckart wave functions are cast in a form in which they are written as a sum of exponentials. In the last row we give the asymptotic normalizations[27] C^2 for each wave function and note these all to be within the range of values given by Lim[22] and Locher and Mizutani.[28] In Fig. 3 we show the behavior of these wave functions in momentum space. There is very little difference among these functions up to $q=2$ fm^{-1}. In the range $q=2$–3 fm^{-1} all the MEC functions are smaller by a factor of 2–3 compared to the NOMEC function. Further out the ECKART3 function drops much more slowly than the EXP functions and inches closer to the ECKART4 function. The two EXP functions drop in magnitude much faster than the other two and show additional secondary maxima in the range of q beyond 4 fm^{-1}. In summary these functions are close to each other at small q but show substantial difference at high q. In the next section we shall discuss the implications of these features on the calculations of the $p+{}^4$He large angle elastic scattering.

TABLE I. The parameters of the overlap functions used in the calculations. C^2 is the asymptotic normalization.

	ECKART4[a,b] (NOMEC)	ECKART3[a] (MEC)	EXP1 (MEC)	EXP2[c] (MEC)
a_1	1.305	1.455	1.402	1.376
a_2	−5.222	−4.364	−5.790	−6.595
a_3	7.832	4.364	8.882	13.563
a_4	−5.222	−1.455	−5.852	−13.161
a_5	1.305		1.358	4.817
β_1	0	0	0	0
β_2	1.42	1.091	1.337	1.42
β_3	2.84	2.182	2.709	2.84
β_4	4.26	3.273	4.358	4.26
β_5	5.68		6.648	5.68
C^2	12.65	15.72	14.6	14.07

[a]The ECKART functions are expanded here as a sum of exponentials [see Eq. (9)].
[b]The parameters are from Ref. 14.
[c]The parameters are from Ref. 24.

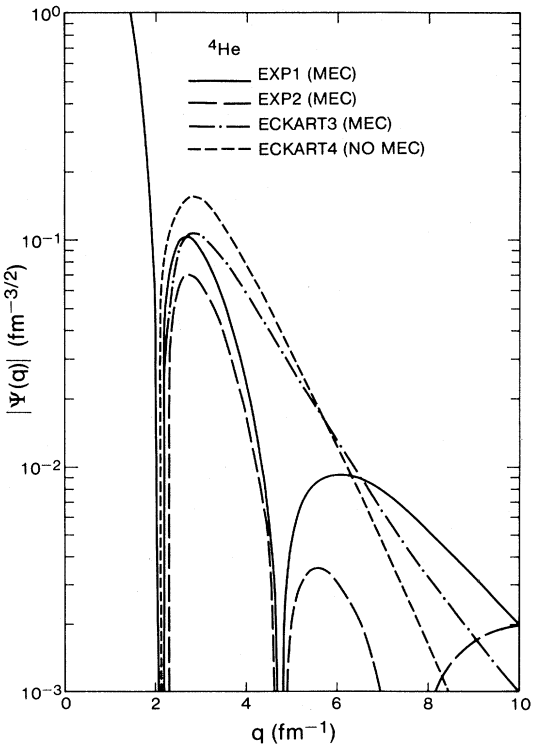

FIG. 3. The ^{4}He overlap wave function $\psi(q)$ in momentum space. The (short-dashed) curve is the function ECKART4 (NOMEC). The (dot-dashed) curve is the function ECKART3 (MEC). The (long-dashed) curve is the function EXP2 (MEC). The (solid) curve is the function EXP1 (MEC).

III. RESULTS AND DISCUSSION

Calculations were performed for p-^{4}He scattering in the energy range 156–800 MeV. The data analyzed here are the cross section data at 156 MeV,[29,30] at 300 MeV,[31] at 200, 350, and 500 MeV,[6] and at 800 MeV.[32] In addition the polarization data at 147 MeV,[29] and at 200, 350, and 500 MeV (Ref. 6) have also been analyzed. The optical potential parameters for 156 and 300 MeV data are taken from Ref. 33. For the other energies these were obtained using the computer search code MAGALI.[34] The differential cross section and polarization data at forward angles ($\theta \leq 85°$) at a given incident energy were analyzed together. Reasonable fits to the data at 200 and 350 MeV were obtained. However, for the data at 500 and 800 MeV, this procedure of simultaneous searches on cross section and polarization did not lead to satisfactory fits to the data. It was possible, nevertheless, to get for each case a reasonably good fit by making separate searches on either the cross section or the polarization data. This resulted in two sets of optical potentials for each of these two cases. When discussing the large angle cross sections for these two energies we shall, therefore, use the set of optical model parameters that best fits the forward cross sections and likewise for polarization. The best fit parameters used in the present analysis are given in Table II.

Lésniak *et al.*[14] have calculated the full exchange amplitude using an eikonal approximation for the distorted waves, but neglecting any contributions from the direct scattering term. In the present work, the direct amplitude is included in the calculations and hence it is possible to assess its effect on the predicted large angle cross section. This point is clarified by the comparison in Fig. 4 where we show the calculations for the large angle cross sections for $T_p = 350$ MeV using the overlap function EXP1. The solid curve represents the calculations using the full amplitude of Eq. (3), i.e., the (OM + HPS) amplitude, while the other two curves are those due to the individual HPS and OM amplitudes. For comparison, the experimental points of Moss *et al.*[6] are shown. Note that the OM result is very low compared to the HPS one at back angles. However, the inclusion of the OM contribution at back angles increases the predicted cross section by roughly a factor of 1.5 at this energy. This indicates that the interference between the two amplitudes is not negligible. Moreover, the combined amplitude calculations are in much better agreement with the data for $\theta > 130°$. It should be noted, however, that the shoulder exhibited by the data around 120° is not reproduced; in fact the interference appears to worsen slightly the agreement with experiment in the

TABLE II. Optical-model parameters for $p + {}^4$He elastic scattering in the energy range 147–800 MeV. $r_c = 1.36$ fm.

T_p (MeV)	V_0 (MeV)	r_0 (fm)	a_0 (fm)	W (MeV)	r_i (fm)	a_i (fm)	$V_{s.o.}$ (MeV)	$r_{s.o.}$ (fm)	$a_{s.o.}$ (fm)	$W_{s.o.}$ (MeV)	r_{iso} (fm)	a_{iso} (fm)
147	6.200	1.560	0.680	12.20	1.540	0.317	7.880	0.802	0.265	−5.090	0.802	0.265
156	8.505	1.359	0.176	11.95	1.554	0.350	5.182	0.840	0.240	−4.031	0.840	0.240
200	2.200	1.560	0.680	14.80	1.540	0.317	4.230	0.802	0.265	−4.420	0.802	0.265
300	2.098	1.063	0.322	24.36	1.342	0.299	4.970	0.821	0.328	−6.448	0.821	0.328
350	−10.566	1.075	0.156	37.87	1.198	0.744	5.650	0.854	0.358	−6.960	0.849	0.315
500[a]	−27.190	1.110	0.101	65.06	1.056	0.284	7.160	0.891	0.252	−7.190	0.887	0.224
500[b]	−11.600	1.025	0.146	64.23	1.158	0.259	2.357	0.830	0.502	−5.699	0.889	0.298
800[a]	−6.835	0.968	0.114	79.01	1.118	0.264	3.797	0.569	0.488	−5.688	0.862	0.287
800[b]												

[a]Best fit to cross section data only.
[b]Best fit to polarization data only.

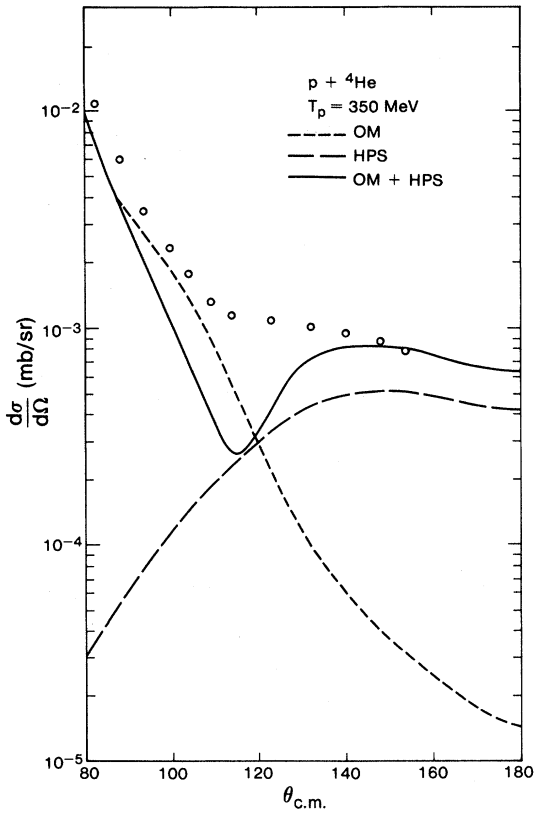

FIG. 4. Large angle $p + {}^4\text{He}$ differential cross section at 350 MeV. The (solid) curve represents the calculations using the full amplitude (OM + HPS). The (short-dashed) and (long-dashed) curves are those due to the individual OM and HPS amplitudes, respectively. The overlap function used is EXP1. The experimental data are from Ref. 6.

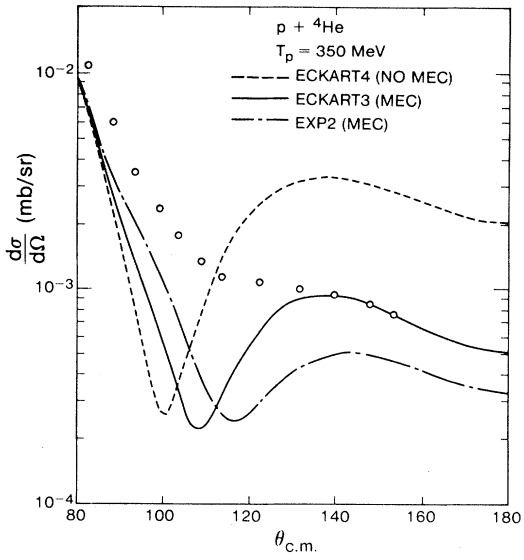

FIG. 5. Large angle $p + {}^4\text{He}$ differential cross section at 350 MeV. The (short-dashed) curve is the full amplitude calculations using the overlap function ECKART4 (NOMEC). The (dot-dashed) curve shows the full amplitude calculations using the function EXP2 (MEC). The (solid) curve represents the full amplitude calculations using the function ECKART3 (MEC). The experimental data are from Ref. 6.

angular range 90°—120°.

Now we would like to discuss the effect of the ^{4}He overlap function on the calculations. Figure 5 shows a comparison of the large angle differential cross sections at $T_p = 350$ MeV using different overlap functions. The dashed curve shows the calculations using the ECKART4 function (NOMEC). The solid and dash-dotted curves are those using ECKART3 and EXP2 functions, respectively, where MEC was taken into account, as discussed in Sec. II. We find large differences among the predicted cross sections and further note that the ECKART3 function yields good agreement with the data for $\theta \geq 140°$, with the EXP2 function faring slightly better near $\theta \sim 100°$ but doing worse elsewhere. The prediction based on the ECKART4 overlap function is the least satisfactory. All three functions produce rather deep interference minima in the $\theta = 100°$—$120°$ region. The observed differences among these calculated cross sections are closely related to the momentum space behavior of the associated overlap functions. Inspection of Fig. 3 shows that in the momentum region of interest (near the second maximum) the ECKART4 function lies highest while the EXP1 and ECKART3 functions almost coincide and the EXP2 function is lowest. These are basically the respective positions of the corresponding back angle cross sections as shown in Figs. 4 and 5.

It is appropriate at this stage to look at the level of accord with experiment over the full angular range and to discuss the effect of the interference between OM and HPS amplitudes at forward angles. Figure 6 shows the full angular distribution of the differential cross section at $T_p = 350$ MeV. The short-dashed curve represents the calculations using the OM amplitude alone, while the long-dashed and solid curves show the calculations using OM + HPS for ECKART4 (NOMEC) and EXP1 (MEC), respectively. It is to be noted that the calculations using OM and OM + HPS are the same up to 85°, indicating that HPS has no effect at forward angles. Note also that, overall, we have a reasonably good agreement with experiment (except for the dip near 120°) when the MEC effects are accounted for. We obtained similar results for the angular distributions at 156 and 500 MeV.

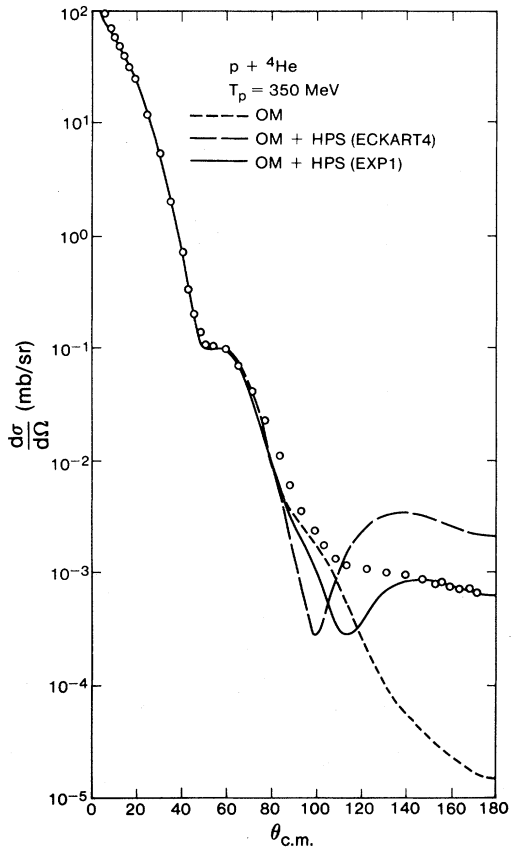

FIG. 6. Full angular distribution of the $p + {}^4\mathrm{He}$ differential cross section at 350 MeV. The (short-dashed) curve is the optical potential (OM) result. The (long-dashed) curve shows the full amplitude calculations using the overlap function ECKART4 (NOMEC). The (solid) curve represents the full amplitude calculations using the function EXP1 (MEC). The experimental data are from Ref. 6.

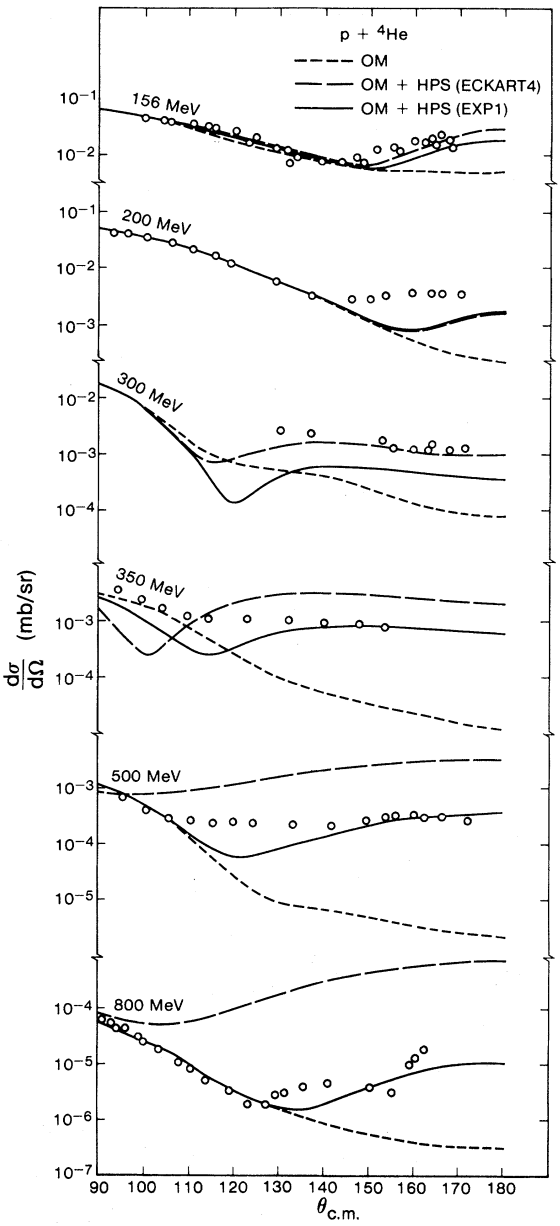

FIG. 7. Large angle $p + {}^4\mathrm{He}$ differential cross sections in the energy range 156–800 MeV. The (short-dashed) curves are the optical potential (OM) results. The (long-dashed) curves show the full amplitude calculations using the overlap function ECKART4 (NOMEC). The (solid) curves represent the full amplitude calculations using the function EXP1 (MEC). The experimental data at 156 MeV are from Refs. 29 and 30, at 200, 350, and 500 MeV from Ref. 6, at 300 MeV from Ref. 31, and at 800 MeV from Ref. 32.

The energy dependence of the cross section at back angles is shown in Fig. 7. The incident proton energies are 156, 200, 300, 350, 500, and 800 MeV. The curves shown are the same as those described in the preceding paragraph. We note the following.

(i) In all cases, the OM calculations invariably underestimate the large angle cross sections.

(ii) Substantial improvement in the accord with the data is obtained when one includes the HPS contribution and when one uses an overlap function (EXP1) which accommodates the effects of meson exchange currents on the charge form factor.

(iii) There is very little difference between the predictions of the ECKART4 (NOMEC) and the EXP1 (MEC) functions at 156 and 200 MeV. These differences become progressively more pronounced as the energy increases, reflecting the greater disparity between these overlap functions at high momenta.

(iv) The ECKART4 calculations do better than the EXP1 calculations at 300 MeV. This, however, is the one case for which the optical potential

parameters were derived from sparse forward angle data and hence may not be very well determined. We, therefore, hesitate to draw any conclusions concerning the relative merit of these two functions at this particular energy.

(v) The calculations at 800 MeV fail to reproduce the observed diffraction minimum near $\theta = 155°$.

We have also investigated the behavior of the differential cross section at $\theta_{c.m.} = 180°$ as a function of the incident proton energy. Figure 8 shows this behavior. The (extrapolated) data points shown are taken from Refs. 5, 10, and 35–41. The dashed and solid curves are obtained using the present model with the overlap functions ECKART4 (NOMEC) and EXP1 (MEC), respectively. Earlier calculations[13,14] have predicted a dip in the energy range 190–240 MeV. We note that, for the case of the ECKART4 function, (i) the calculated cross section has a dip at about 280 MeV, and (ii) the calculated cross section is in good agreement with the data points up to 300 MeV; above this energy the calculations are rather high compared to the data. On the other hand, for the EXP1 function we notice the following: (i) the calculated cross section is in good qualitative agreement with the data points over all the energy range, and (ii) the calculations show two dips, one near 300 MeV and the other near 950 MeV. The appearance of these dips at these particular energies is closely related to the behavior of the overlap function $\Psi(q)$ of Fig. 3, where we notice that ECKART4 has one dip while EXP1 has two dips for $q \leq 10$ fm^{-1}. Berthet *et al.*[4] have measured the p-^{3}He elastic backward scattering cross section in the energy range $700 \leq T_p \leq 1700$ MeV. They found a change in the slope of the cross section ($\theta_{c.m.} = 180°$) at about 500 MeV and a bump at about 1300 MeV. They explained these features as due to baryonic excitations in intermediate states.

Now we focus our attention on polarization. Figure 9 shows the complete angular distribution for the polarization at $T_p = 350$ MeV. The data shown are those of Moss *et al.*[6] The solid curve represents the calculations using the (OM + HPS) amplitudes and the overlap function EXP1. The short- and long-dashed curves represent the calculations using the individual OM and HPS amplitudes, respectively. Note that the OM and OM + HPS calculations are the same up to 90°. The effect of the inclusion of the HPS term becomes noticeable in the angular range 120°–180°. Note also that in this region the HPS and HPS + OM predictions are both consistently negative, which is qualitatively what the data show. However, it is clear that a detailed

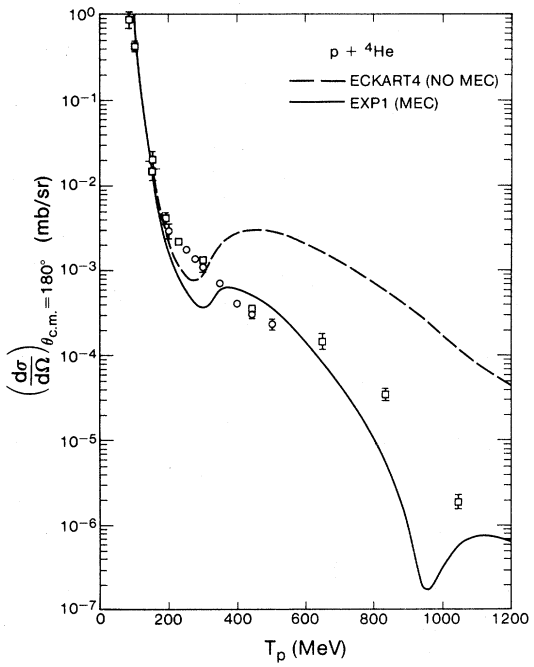

FIG. 8. The p-^{4}He elastic scattering cross section (at $\theta_{c.m.} = 180°$) as a function of incident proton energy. The dashed curve shows the full amplitude calculations using the overlap function ECKART4 (NOMEC). The solid curve represents the full amplitude calculations using the function EXP1 (MEC). The optical model parameters used in the calculations are from Table II and Ref. 33. The experimental data: open circles are from Ref. 5; the squares are from Refs. 10 and 35–41.

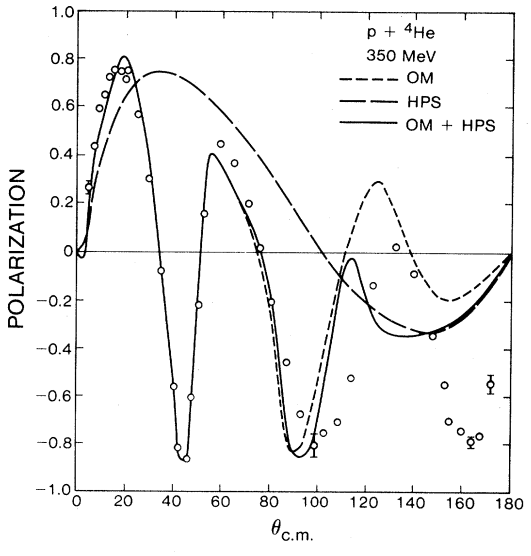

FIG. 9. Polarization in p + ^{4}He scattering at 350 MeV. The (short-dashed) curve is the optical potential (OM) result. The (long-dashed) curve shows the HPS result. The (solid) curve represents the full amplitude calculations. The overlap function used is EXP1 (MEC). The experimental data are from Ref. 6.

agreement with this large angle data is lacking. The back angle distribution for polarization in the energy range 147–500 MeV is shown in Fig. 10. The data points at 147 MeV are taken from Ref. 29 and those of 200, 350, and 500 MeV are taken from Ref. 6. The short-dashed curve represents the calculations using the OM amplitude. The long-dashed and solid curves represent the calculations using OM + HPS amplitudes with the overlap functions ECKART4 (NOMEC) and EXP1 (MEC), respectively. It should be noted that, with either function, the agreement between experimental data and the OM + HPS calculations at $T=147$ MeV is reasonably good. As the incident energy is increased we find that the inclusion of the HPS contribution does not lead to any consistent improvement in the calculated polarizations. Specifically, we note that at 200 MeV there is actually some worsening in the accord with the data near $\theta=100°$, with only small differences between the ECKART4 (NOMEC) and the EXP1 (MEC) predictions. At 350 MeV, the ECKART4 calculations are worse than the OM calculations near $\theta=100°$, whereas the EXP1 calculations are only marginally better than the latter. On the other hand, at $T_p=500$ MeV, these same ECKART4 calculations do better than the other two calculations in the angular range 90°–120°. None of the above calculations predicts the correct polarization for $\theta \geq 150°$ for the three proton energies mentioned above. Thus, aside from the 147 MeV case, the situation for polarization remains unclear.

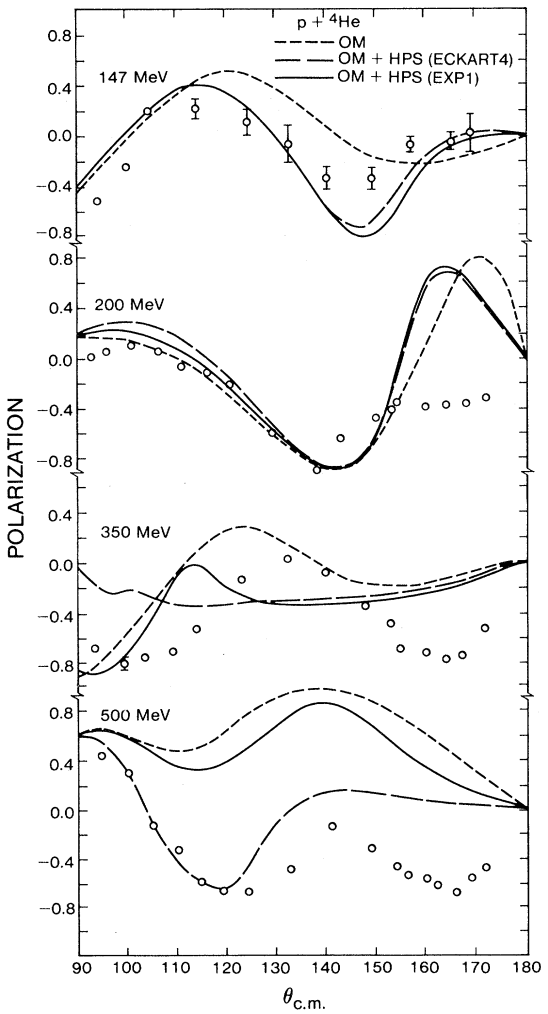

FIG. 10. Large angle polarization in $p + {}^4\text{He}$ scattering in the energy range 147–500 MeV. The (short-dashed) curves are the optical potential (OM) results. The (long-dashed) curves show the full amplitude calculations using the overlap function ECKART4 (NOMEC). The (solid) curves represent the full amplitude calculations using the function EXP1 (MEC). At 147 MeV the experimental data are from Ref. 29; at 200, 350, and 500 MeV they are from Ref. 6.

IV. CONCLUSION

In this paper we have described a simple model for treating particle exchange effects in the elastic scattering of nucleons on light nuclei with particular emphasis on large angle scattering. The thrust of this investigation is to see how far one can go without introducing exotic effects such as Δ resonances, etc., and if one can in fact learn anything useful about the target wave function. The main ingredient of the present approach is that the scattering amplitude is approximated by the sum of an optical potential amplitude and a heavy particle stripping amplitude. The latter represents the part of the exchange amplitude likely to dominate at large angles and is calculated using a distorted-wave Born approximation. The model has been applied here to $p + {}^4\text{He}$ scattering at intermediate energy. Target overlap functions derived from electron scattering data (with and without allowance for meson exchange current effects) have been used in the calculations. We have found that the calculated large angle cross sections are sensitive to the large momentum behavior of the overlap function. Large differences among the several wave functions investigated here at high momentum were reflected in large differences in the corresponding back angle cross section. Moreover, we have found that the results obtained with wave functions which take into account the meson exchange corrections to the charge form factor are generally in better agreement with the data than the wave function that does not. The difference is more pronounced at higher energies. From this one concludes that one must take MEC contributions into account when dealing with pro-

cesses involving large momentum transfer. The general behavior of the large angle cross section in the energy range 0.1—0.8 GeV is reproduced by our calculations particularly when the wave function EXP1 is used. This makes one hope that eventually large angle $p + {}^4$He scattering can play a role in probing the large momentum behavior of the ^{4}He wave function. We have also obtained good qualitative agreement with the 180° excitation function up to ~ 0.8 GeV, when the MEC corrected wave function EXP1 is used. In contrast, the ECKART4 wave function deviates appreciably from the data for $T_p > 0.4$ GeV, again an indication of the importance of the MEC corrections. One interesting result of the present calculations is the appearance of a second dip in the excitation function near 1 GeV. An experimental check of this feature would be highly desirable. We note here that a similar feature has already been observed experimentally by Berthet *et al.*[4] for the case of $p + {}^3$He scattering.

Our simple model, however, does not do as well for polarization as it does for the cross section. We can only claim some improvement for large angle polarization at $T_p = 147$ MeV. At the other three energies considered, one still does not successfully account for the observed large angle polarizations. This may indicate that the model requires further refinements. One natural improvement upon the present method is to actually invoke the HPS contribution while one is attempting to determine the parameters of the optical potential. This may ultimately lead to improved results for the cross section near the interference region as well as for the large angle polarization. Because the HPS calculations are rather complicated, this would naturally be a lengthy computation but, nevertheless, one which we hope to be able to do in the near future.

Recently Kowalski[42] developed a formal treatment of the optical potential in which Pauli effects are taken into account. He has shown that in lowest order the full potential contains a heavy particle stripping term. A calculation using this type of full optical potential would be interesting to compare with the results of our present model and with the experimental data. We remark that if one chooses to treat the contribution of the HPS term in the potential in a DWBA framework, then the resulting amplitude will be slightly different from that given by Eq. (4). In particular, the plane wave in Eq. (4) will have to be replaced by an appropriate distorted wave. On the other hand, we note that, as pointed out in Sec. I, Greenlees and Tang[9] have suggested the use of Majorana exchange terms in the potential to simulate the exchange effects. This may be regarded as a specific simplified version of the result given by Kowalski. Such simple phenomenological potentials have been used in the analysis of the scattering data (see, for example, Refs. 24 and 33).

One criticism of our model is the way it handles the knockout amplitude, which is here assumed to be well represented together with the direct amplitude by the optical potential amplitude. It is possible that the knockout amplitude may have important contributions at large angles which may not be accounted for by the $T_{\rm OPT}$. In this connection we wish to mention the work of Alexander and Landau,[43] who have carried out a microscopic calculation of the p-^{4}He optical potential in which the full angular behavior of the elementary N-N amplitudes was taken into account. Their initial results for the cross section data in the energy range $T_p = 100$—200 MeV were rather encouraging. A detailed calculation along these lines, with application to data at higher energies, is extremely desirable.

In a forthcoming publication the case of $p + {}^3$He scattering will be discussed.

ACKNOWLEDGMENTS

The authors wish to thank J. Greben and J. Shepard for providing us with details of their work on the overlap functions and J. Raynal for a copy of the search code MAGALI. We are grateful to the late John S. Blair for many useful discussions. One of the authors (H.S.S.) wishes to thank the Nuclear Theory group at the University of Washington for their hospitality during the academic year 1979—1980, when parts of this work were completed. Another of us (M.S.A.) is grateful to the Nuclear Research Centre, University of Alberta for their hospitality and to the University of Petroleum and Minerals for financial support. This work was supported in part by Natural Science and Energy Research Council of Canada and by the U.S. Department of Energy.

*Permanent address: Nuclear Research Centre, University of Alberta, Edmonton, Alberta, Canada T6G 2N5.

†Permanent address: University of Petroleum and Minerals, Dhahran, Saudi Arabia.

‡Present address: Defense Research Establishment Pacific, B.C., Canada.

[1] E. D. Cooper and H. S. Sherif, Phys. Rev. Lett. 47, 818 (1981); Phys. Rev. C 25, 3024 (1982).

[2]E. Rost, J. R. Shepard, and D. Murdock, Phys. Rev. Lett. 49, 448 (1982).
[3]G. Igo, Nucl. Phys. A374, 253c (1982).
[4]P. Berthet, R. Frascaria, B. Tatischeff, J. Banaigs, J. Berger, J. Duflo, L. Goldzahl, F. Plouin, F. Fabbri, P. Picozza, M. Boivin, and L. Satta, Phys. Lett. 106B, 465 (1981).
[5]R. H. McCamis, J. M. Cameron, L. G. Greeniaus, D. A. Hutcheon, C. A. Miller, G. A. Moss, G. Roy, M. S. de Jong, B. T. Murdoch, W. T. H. van Oers, J. G. Rogers, and A. W. Stetz, Nucl. Phys. A302, 388 (1978).
[6]G. A. Moss, L. G. Greeniaus, J. M. Cameron, D. A. Hutcheon, R. L. Liljestrand, C. A. Miller, G. Roy, B. K. S. Koene, W. T. H. van Oers, A. W. Stetz, A. Willis, and N. Willis, Phys. Rev. C 21, 1932 (1980).
[7]A. Herzenberg and E. J. Squires, Nucl. Phys. 19, 280 (1960).
[8]D. R. Thompson, R. E. Brown, M. Lemere, and Y. C. Tang, Phys. Rev. C 16, 1 (1977); I. Reichstein and Y. C. Tang, Nucl. Phys. A158, 529 (1970).
[9]G. W. Greenlees and Y. C. Tang, Phys. Lett. 34B, 359 (1971).
[10]L. G. Votta, P. G. Roos, N. S. Chant, and R. Woody III, Phys. Rev. C 10, 520 (1974); V. Comparat, R. Frascaria, N. Fujiwara, N. Marty, M. Morlet, P. G. Roos, and A. Willis, *ibid.* 12, 251 (1975).
[11]B. S. Podmore and H. S. Sherif, in *Few Body Problems in Nuclear and Particle Physics,* edited by R. J. Slobodrian *et al.* (Laval University, Quebec, 1975), p. 517.
[12]L. G. Arnold, B. C. Clark, and R. L. Mercer, Phys. Rev. C 21, 1899 (1980).
[13]B. Z. Kopeliovich and I. K. Potashnikova, Yad. Fiz. 13, 1032 (1971) [Sov. J. Nucl. Phys. 13, 592 (1971)].
[14]H. Lésniak, L. Lésniak, and A. Tekou, Nucl. Phys. A267, 503 (1976).
[15]H. S. Sherif and R. S. Sloboda, Phys. Lett. 99B, 369 (1981).
[16]M. L. Goldberger and K. M. Watson, *Collision Theory* (Wiley, New York, 1964), p. 153.
[17]L. Madansky and G. E. Owen, Phys. Rev. 99, 1608 (1955); N. Austern, *Direct Nuclear Reaction Theories* (Wiley, New York, 1970), p. 339.
[18]G. R. Satchler, in *Lectures in Theoretical Physics,* edited by P. D. Kurz, D. A. Lind, and W. E. Brittin (The University of Colorado, Boulder, 1966), p. 73.
[19]E. V. Ivash and R. J. Kulkarni, Phys. Rev. C 14, 2063 (1976).
[20]R. F. Frosch, J. S. McCarthy, R. E. Rand, and M. R. Yearian, Phys. Rev. 160, 874 (1967).
[21]R. G. Arnold, B. T. Chertok, S. Rock, W. P. Shütz, Z. M. Szalata, D. Day, J. S. McCarthy, F. Martin, B. A. Mecking, I. Sick, and G. Tamas, Phys. Rev. Lett. 40, 1429 (1978).
[22]T. K. Lim, Phys. Lett. 44B, 341 (1973).
[23]J. R. Shepard, E. Rost, and G. R. Smith, Phys. Lett. 89B, 13 (1979).
[24]W. T. H. van Oers, B. T. Murdoch, B. K. S. Koene, D. K. Hasell, R. Abegg, D. J. Margaziotis, M. B. Epstein, G. A. Moss, L. G. Greeniaus, J. M. Greben, J. M. Cameron, J. G. Rogers, and A. W. Stetz, Phys. Rev. C 25, 390 (1982).
[25]M. Gari, H. Hyuga, and J. G. Zabolitzky, Nucl. Phys. A271, 365 (1976).
[26]J. M. Greben, Phys. Lett. 115B, 363 (1982).
[27]T. K. Lim, Phys. Lett. 55B, 252 (1975).
[28]M. P. Locher and T. Mizutani, Phys. Rep. 46, 43 (1978).
[29]A. M. Cormack, J. N. Palmieri, N. F. Ramsey, and R. Wilson, Phys. Rev. 115, 599 (1959); J. N. Palmieri, R. Goloskie, and A. M. Cormack, Phys. Lett. 6, 289(E) (1963).
[30]V. Comparat, R. Frascaria, N. Fujiwara, N. Marty, M. Morlet, P. G. Roos, and A. Willis, Phys. Rev. C 12, 251 (1975).
[31]O. Chamberlain, E. Segré, R. D. Tripp, C. Wiegand, and T. Ypsilantis, Phys. Rev. 102, 1659 (1956).
[32]J. Fong, T. S. Bauer, G. J. Igo, G. Pauletta, R. Ridge, R. Rolfe, J. Soukup, C. A. Whitten, Jr., G. W. Hoffmann, N. Hintz, M. Oothoudt, G. Blanpied, R. L. Liljestrand, and T. Kozlowski, Phys. Lett. 78B, 205 (1978).
[33]S. W. L. Leung and H. S. Sherif, Can. J. Phys. 56, 1116 (1978).
[34]J. Raynal (private communication).
[35]J. Berger, J. Duflo, L. Goldzahl, F. Plouin, F. L. Fabbri, P. Picozza, L. Satta, C. LeBrun, D. Legrand, and J. Oostens, in *Seventh International Conference on High Energy Physics and Nuclear Structure,* edited by M. Locher (Birkhauser, Basel, 1978).
[36]B. W. Davies, M. K. Craddock, R. C. Hanna, Z. J. Moroz, and L. P. Robertson, Nucl. Phys. A97, 241 (1967).
[37]N. D. Goldstein, A. Held, and D. G. Stairs, Can. J. Phys. 48, 2629 (1970).
[38]E. Aslanides, T. Bauer, R. Bertini, R. Beurtey, A. Boudard, F. Brochard, G. Bruge, A. Chaumeaux, H. Catz, J. M. Fontaine, R. Frascaria, D. Garreta, P. Gorodetzky, J. Guyot, F. Hibou, D. Legrand, M. Matova, Y. Terrien, J. Thirion, and E. Lambert, Phys. Lett. B68, 221 (1977).
[39]J. Berger, J. Duflo, L. Goldzahl, F. Plouin, J. Oostens, M. van den Dossche, L. Vu Hai, G. Bizard, C. LeBrun, F. L. Fabbri, P. Picozza, and L. Satta, Phys. Lett. B63, 111 (1976); Phys. Rev. Lett. 37, 1195 (1976).
[40]S. L. Verbeck, J. C. Fong, G. Igo, C. A. Whitten, Jr., D. L. Hendrie, Y. Terrien, V. Perez-Mendez, and G. W. Hoffmann, Phys. Lett. B59, 339 (1975).
[41]P. G. McManigal, R. D. Eandi, S. N. Kaplan, and B. J. Moyer, Phys. Rev. 137, B620 (1965).
[42]K. L. Kowalski, Phys. Rev. C 25, 700 (1982).
[43]Y. Alexander and R. H. Landau, Phys. Lett. 84B, 292 (1979).